

Pandemic Mitigation: the Basic Reproduction Number

JAY BORIS

*Chief Scientist
Material Science and Component Technology Directorate*

KEITH OBENSCHAIN

*Head, Laboratory for Advanced Computational Physics
Laboratories for Computational Physics and Fluid Dynamics*

DAVID BORIS

*Technical Collaborator
Webster New York*

November 26, 2021

This page intentionally left blank.

1. A Brief Description of the PANDEMIC Model

“The inevitable, but unpredictable, appearance of new infectious diseases has been recognized for millennia, well before the discovery of causative infectious agents. Today, however, despite extraordinary advances in development of countermeasures (diagnostics, therapeutics, and vaccines), the ease of world travel and increased global interdependence have added layers of complexity to containing these infectious diseases that affect not only the health but the economic stability of societies. HIV/AIDS, severe acute respiratory syndrome (SARS), and the most recent 2009 pandemic H1N1 influenza are only a few of many examples of emerging infectious diseases in the modern world; each of these diseases has caused global societal and economic impact related to unexpected illnesses and deaths, as well as interference with travel, business, and many normal life activities. Other emerging infections are less catastrophic than these examples; however, they nonetheless may take a significant human toll as well as cause public fear, economic loss, and other adverse outcomes” (Morens and Fauci, 2013).

More realistic models of epidemic spread are needed to estimate the effects of social and governmental policy. Some epidemic models are statistical in nature, trying to interpolate and apply curves adapted from previous epidemics. However, the characteristics of viral transmission, incubation and susceptibility vary between diseases, putting modelers at a disadvantage in an ongoing epidemic where these parameters are unknown. Further, “The sparsity of such events (i.e. pandemics) and changes in outbreak recording, may make identifying suitable validation data difficult.” (Walters, et al., 2018) Other modeling approaches try to approximate individual interactions according to representations that break populations into broad classes or categories relative to their susceptibility or mobility. Yet other approaches try to treat the problem more atomically as a modified form of molecular dynamics. A “simple model makes a gallon of faulty assumptions – including that human beings move around and contact one another randomly, like molecules in a gas, instead of making very nonrandom contacts within certain networks, as we actually do. You are much more likely to contact a specific group of folks in your local community, whether at your workplace, wherever you worship or in your own household.” (William Hanage and Helen Jenkins, 2020) None of the statistical and lumped-parameter models can be very realistic in a new situation because of the importance of human behavior in the virus transmission rate.

Figure 1 is an instantaneous population-map graphic from the PANDEMIC detailed simulation model. It shows the model’s current geographic coverage area, the Washington DC Metropolitan region. This metro region has a population estimated at over 6 million people, which makes it the 7th largest metropolitan area in the United States. In PANDEMIC, the metro region around Washington DC and Baltimore is taken as a 100 km by 100 km square. The portions of Maryland and Virginia outside this region are mostly rural with low population densities and 6.25 million people is a little over 40% of the combined populations of the two states. These numbers approximate what must be the correct for this square region. Getting a good estimate of the total number of people in the area involved alleviates the need to scale results up from much smaller populations when so much about the transmission interactions and effect of mitigation procedures depends on the number of people each person interactions with.

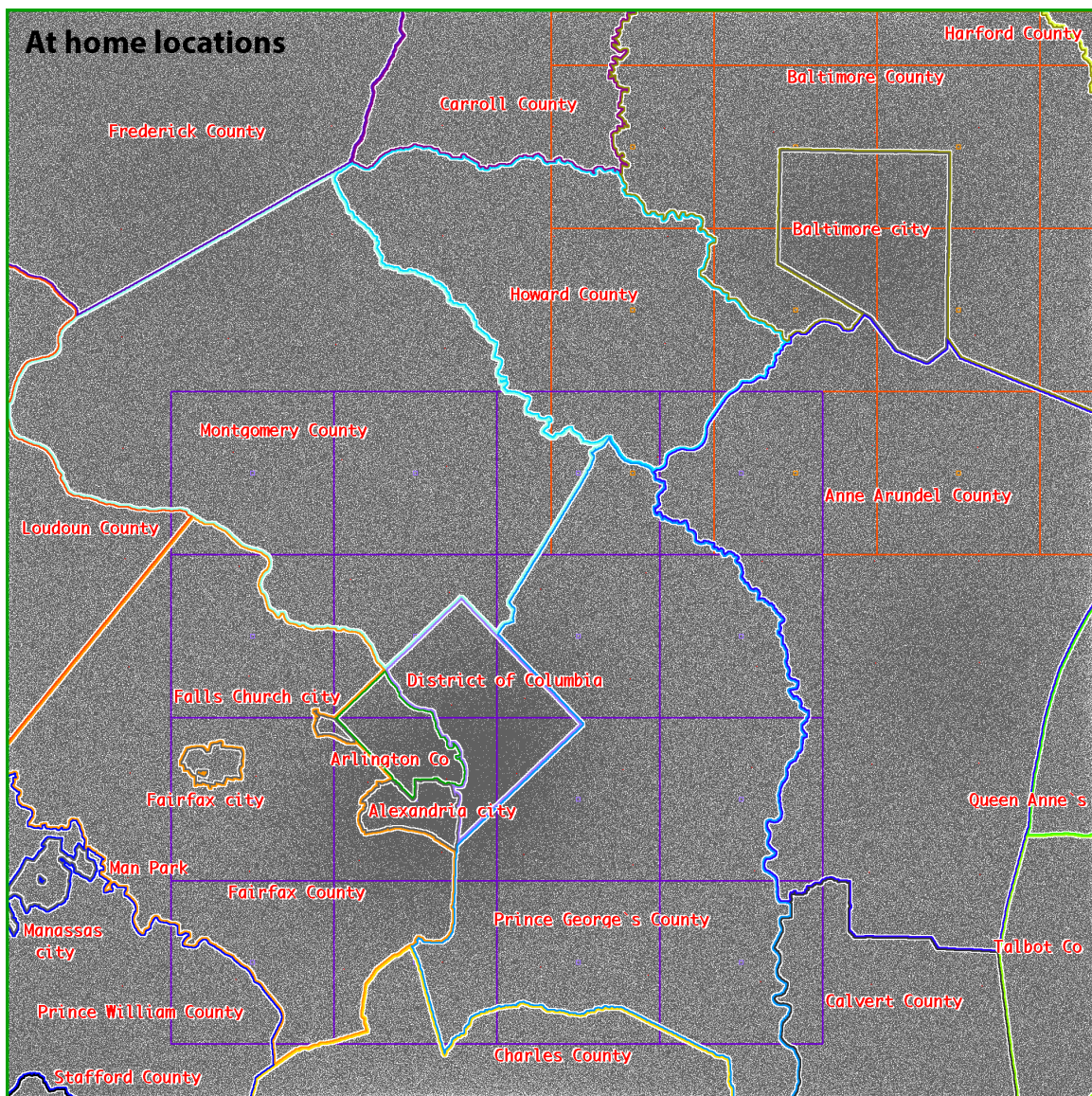


Figure 1. Home locations of 6.25 million people in NRL's PANDEMIC simulation model approximating the Washington DC Metro region. These homes are arranged in a 2500 x 2500 Monotonic Lagrangian Grid (MLG) to efficiently compute the near-neighbor exposures to the virus as the people move about. The grey pixel density shows the population density when everyone is at home.

Figure 1 visualizes the initial condition of PANDEMIC simulations aimed at studying the Covid-19 pandemic as it has evolved in this region from mid-March 2020 to the present. The Maryland and Virginia county boundaries and the several separately incorporated cities are shown but the numbers of people within each county only approximate the actual numbers and no effort is made to simulate the actual specific people. In the initial setup in March 2020, 81 infected people were randomly distributed around the metro region. These original Covid-19 carriers, assumed still to be asymptomatic but contagious, are represented by isolated red pixels scattered about the figure. More red pixels are visible later in time in the insets of Figs. 5 and 6 in Pandemic Report #1 (Boris, Obenschain, and Boris, 2021a). Each pixel in Fig. 1 covers a 50 x 50 meter square on a 2000 x 2000 plotting grid so several people must often be plotted at the same pixel. Choosing 81 contagious people initially provides a few seeds for the virus to grow while not swamping the region with a large number of initial sources. On March 14th 2020, according

to *worldometer*, there were 4279 Covid-19 cases in the United States. The initial 81 covid contagious people in PANDEMIC is $4279 \times 6.25 \text{ million} / 330 \text{ million}$, a proportionate number.

PANDEMIC is not a lumped parameter or regionally averaged representation and it is not a 'molecular dynamics' algorithm where the people move about randomly and bump into each other to interact. The model is also not based on statistical extrapolations from a detailed database of cases. PANDEMIC more closely resembles an earlier Discrete Simulation Monte Carlo model using the MLG (Cybyk, et al., 1994 & 1995). The simulated people in PANDEMIC all have different personal parameters and live in different places. These people each follow realistic movement and behavior patterns that vary throughout the day and week. A summary of Covid-19 data and research available in April 2020 was used to implement a simple contagious-transmission model that depends on time in proximity and inter-personal separation. A mask efficiency factor M_{eff} , and an age-based demographic model of probability of fatality are included (D. Boris, 2020; L. Bourouiba, 2020; V. Vuorinen, et al., 2020; L. Bourouiba, et al., 2014; California Covid Deaths by Age, 2020).

The current version of the model treats the idealized region shown in Fig. 1 including Washington DC, Baltimore, Annapolis and Frederick in Maryland, and Alexandria, Fairfax City, and Reston in Virginia, as shown below. The grey dots in the figure show the approximate at-home locations of the 6.25 million people, laid out on a 2500 by 2500 Monotonic Lagrangian Grid. The cities appear as darker local population concentrations where the pixels representing people are clustered more closely in the urban and suburban areas. This approximation to geographic fidelity could be improved appreciably given more time and resources. The current treatment, however, provides an improvement over more homogeneous historical or data-based models and affords opportunities to study the effects that differences in behavior patterns and proximity, both personal and mandated, will have on the evolution of an epidemic.

This development effort was spurred by the Covid-19 pandemic presently sweeping the earth. The goal of the PANDEMIC effort was to provide a fast but accurate simulation model allowing analysis of some of the complexities and possible mitigation strategies for the current corona virus epidemic. Parameters for the virus simulation such as incubation time, viral susceptibility vs age, and death probability, where possible, are estimated using data from Covid-19. This model has the potential to accurately assess the effects of behaviors in large populations that cannot be captured either due to the smaller size scales of these simulations or their inability to reflect realistic human behaviors. PANDEMIC was developed and tested using optimized parallel-programming algorithms for advanced new architectures. For example, these runs execute more than 2000 times faster than real time on a multi-core laptop while predicting reasonable rise and decay times for infection as the pandemic progresses.

This report does not provide a very detailed specification of the PANDEMIC model, its algorithms or its programming. Two earlier reports (Boris, Obenschain, and Boris, 2021a & 2021b), though not intended as detailed model documentation, contain much additional information and related references. Information about the effects and time-scales for the action of Covid-19 as a function of population demographics is still being understood and is changing with time. Further, how this model should evolve is not ready to be 'cast in concrete.' The ability to try combinations of parameters and vary the underlying models representing the action of the disease has allowed us to calibrate PANDEMIC to existing data when available, for reasonable validation. PANDEMIC implements several interacting mitigation strategies to test individually

and in concert how much of an effect on the epidemic can be expected. These strategies include social distancing, isolation or confinement once symptoms (or the virus) have been diagnosed, wearing of masks during close interactions with the potential for infection, and teleworking to meetings, church, and the workplace. Results of these simulations and comparisons are reported here and the earlier two reports.

Each simulated person is assigned a random age from a demographic probability distribution, available from gathered data. Each person's susceptibility, also randomly assigned, drives their mortality under Covid-19 to closely approximate the population average for the person's age. These are not intended to be specific people but rather to approximate the general population distributions reasonably. Separate economic, gender, race, ethnicity, and comorbidity factors are not considered, though these complicating factors could be included with significant additional work. Each person has a changing viral load $V_L(t)$, expressing the absence or extent of the virus in their system, with a continuous value from 0.0 to 4.0. This value is updated by an 'exposure' subroutine using discrete timesteps, typically five times an hour. Different ranges of the viral load are associated with different stages of the Covid-19 infection. These are plotted in the graphical displays from Fig. 2 onward that are produced by PANDEMIC and are described below.

Each person has a critical V_L value, based on their age and susceptibility. At this critical value, V_L begins to decrease due to assumed natural or treatment-induced immunity. The person may pass back down through the contagious range, possibly infecting others, until the person becomes non-contagious. There is still a serious shortage of information about how this all works for Covid-19, so PANDEMIC, like other detailed models that aim to be predictive, makes a host of assumptions, many of which may be faulty, while actual data is being collected about the virus. If a person's critical V_L value, where cure/immunity would begin, is 3.8 or larger, the person dies, retaining his viral load but no longer interacting with others within the simulation.

Holding behavioral and environmental parameters fixed during a scenario is not a requirement of the model, but doing so allows evaluation of the impact of changes in behavior and confinement restrictions alone upon the number of infections and fatalities and on computing the basic reproductive number R_0 from first principles in circumstances where changes in behavior, confinement restrictions and other societal mandates cannot interact with the determination of R_0 . But we begin, in Section 2 below, with a simulation, illustrating the full range of PANDEMIC's capabilities that does not hold behavioral and environmental parameters fixed.

2. A Year-Long PANDEMIC Simulation of the Covid-19 Pandemic

The initial PANDEMIC Report (Boris, Obenschain, and Boris, 2021) studied personal mitigation techniques for the Covid-19 pandemic in the Washington DC Metro region. Simulations there predicted the 3 Covid-19 infection surges observed through February 2021. Different levels of testing to mitigate the 'third surge' were then compared. The year-long baseline case from that study, Scenario 1a, is the starting point for research here on the "basic reproduction number" R_0 , a commonly-used public health metric to evaluate the threat posed by an epidemic. Figure 2 shows the two main diagnostic plots from the PANDEMIC simulation of that baseline scenario.

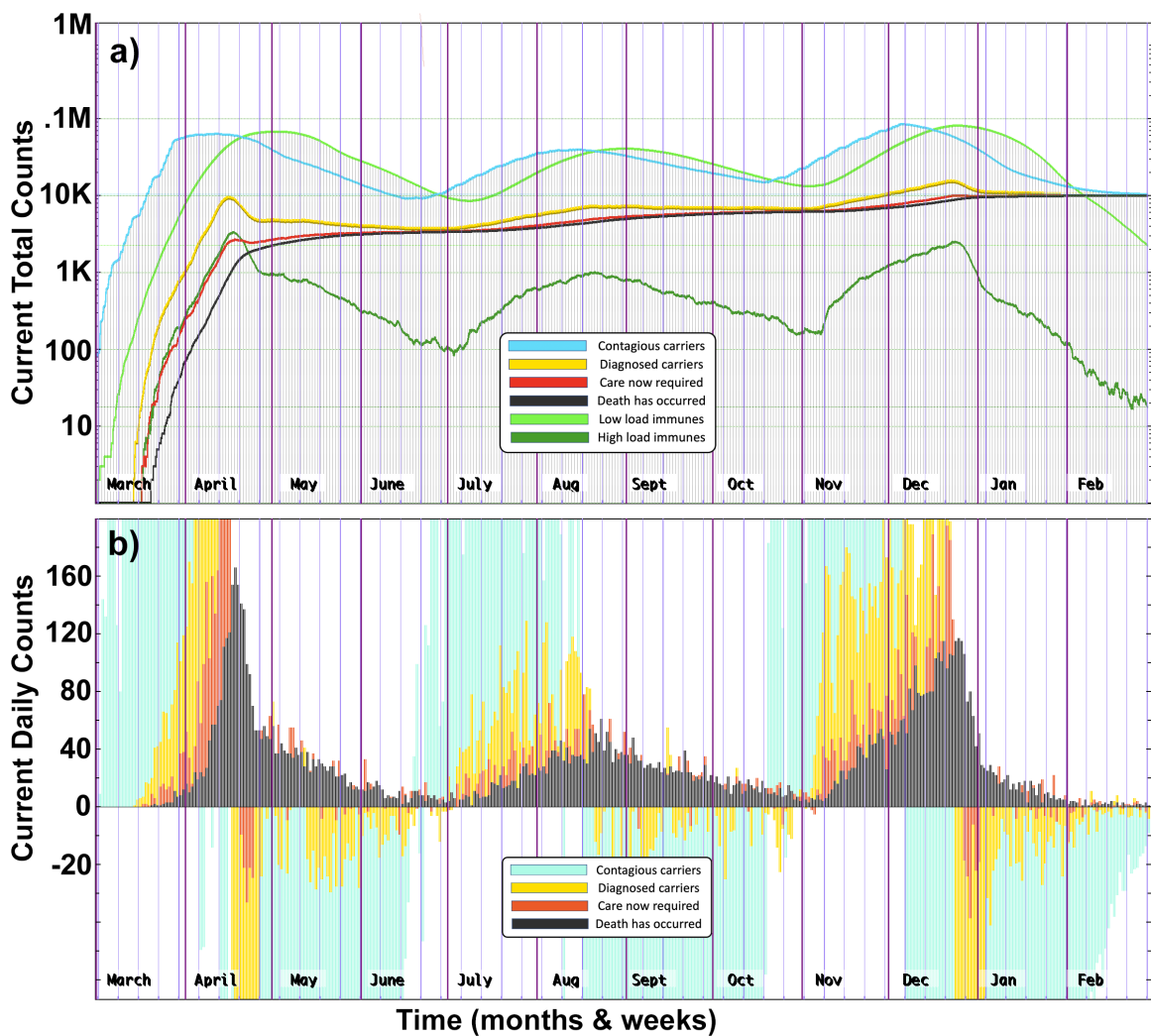


Figure 2. Scenario 1a, 3-surge simulation of the pandemic in the Washington DC Metro area. Panel a) the total number of counts (i.e., people in various stages of infection) of six quantities at each time in a PANDEMIC simulation. Panel b), the current daily counts if the four viral load conditions on a linear scale.

Although the DC Metro region has only 6.25 million people, about 2% of the nation's population, the three Covid-19 surges in the U.S. are clearly reproduced by PANDEMIC in this limited region. The current daily counts are evaluated six times each day. Panel a) plots these data, the current number of contagious carriers of the virus over the entire region (light blue, $V_L(t) \geq 1.0$), diagnosed carriers (yellow, $V_L(t) \geq 2.5$), dangerously infected people with care required (red, $V_L(t) \geq 3.0$), and Covid-19 fatalities (black, $V_L(t) \geq 3.8$). These four infection-level counts become progressively smaller as the viral load values defining each successive level increase. After each infection has run its course either to death or to recuperation, the blue curve must decrease until it joins the increasing black fatality curve, as seen in Panel a) of Fig. 2. The two additional green curves in panel a display two levels of immunity for recovering people as their viral load $V_L(t)$ decreases after peaking at a value below the fatal value 3.8. Panel b) plots the daily differences of these four different infection conditions on a linear scale. This is the presentation format most often used in public reporting. Note that our method of counting results in negative daily counts when the region has decreasing infection totals.

The remainder of this third PANDEMIC report addresses the basic reproduction number R_0 , an epidemiologic metric often used to characterize the progress of an epidemic, in the context

of measuring the stability of the system to the spread of the contagion. R_0 is discussed and its computation is detailed in Section 3 immediately below. First, however, we illustrate the behavior of $R_0(t)$ using the definition in Eq. (1) and explained below, for an alternate interpretation of Scenario 1a visualized in Fig. 2 above. Figure 3 below plots $R_0(t)$, intrinsically a time dependent metric, for the complex Scenario 1a. Seven different tabulation time spans are used to evaluate R_0 , as explained in the following section. These different tabulation spans display different facility in reacting to rapid changes in the scenario resulting from people's changing attitudes and their government's adapting response.

This introductory scenario is perhaps too complicated for good research on R_0 but it serves to illustrate plausible responses to the population's evolving concerns about the brewing pandemic. Assume some forewarning of potential problems to come when a number of people, some likely to be carrying the infection, are injected into the unexposed population. The immediate official response is that businesses and workplaces are told to obey extended telework and this is continued at changing levels throughout the 52 weeks of the scenario. However, meetings were not heavily restricted initially with church and medium scale public meetings initially unrestricted. After two weeks of unrestricted meetings, however, the growing number of cases being detected called for more draconian measures. The people are told to isolate themselves in their homes, respect 2-meter social distancing, and attend no public meetings, at least until the rising pandemic abates significantly.

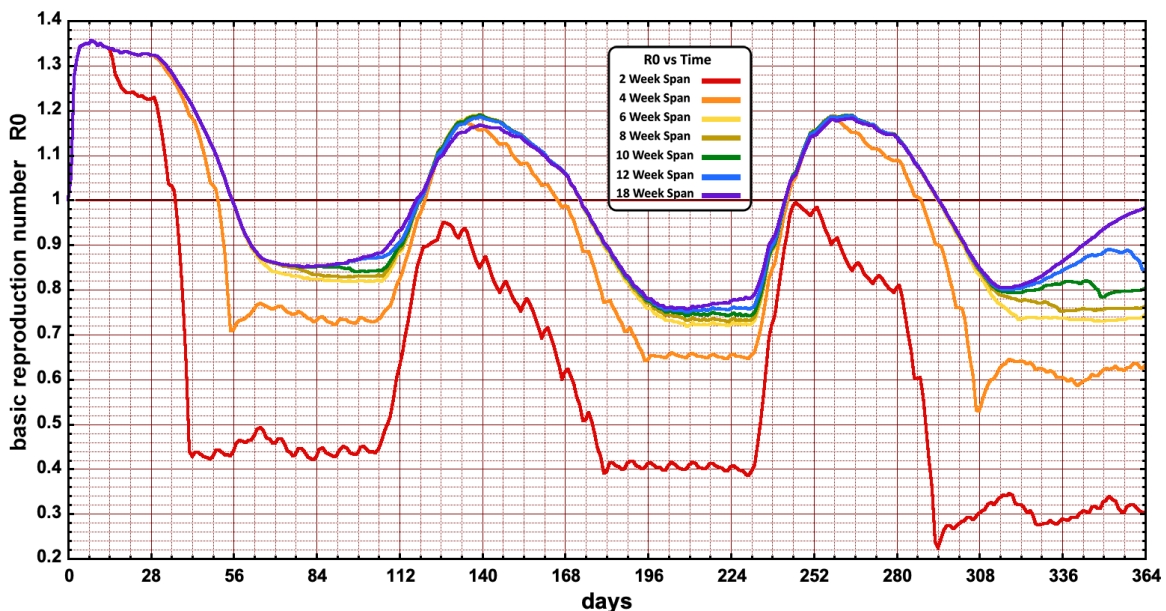


Figure 3. Basic reproduction number R_0 vs time for 52-week 3-surge PANDEMIC simulation (Scenario 1a from PANDEMIC #1). R_0 is computed every day at midnight using 7 different tabulation time spans from 2 weeks to 18 weeks. The solutions using 6-, 8- and 10-week tabulation spans are essentially the same.

After 13 or 14 weeks into Scenario 1a, the incidence of new cases and deaths seems to have abated greatly and pressures to open up the economy have escalated, armed by the good news. Many businesses have found that teleworking, even at the 90% level, has not greatly hampered their productivity and the workers appreciate the time saved by not commuting – often a couple of hours a day. Thus the heavy telework level is continued. Churches and meetings allow virtual/telework possibilities so they open with 50% virtual attendance, hoping that this restriction, coupled with 2-meter social distancing, will avert a return to pandemic-level

infections. After week 14, as it becomes clear that cases of infection and deaths have begun to skyrocket again. Many churches switch to 100% virtual sessions/services. The second surge abates in the autumn and people begin to chafe at the restrictions again. As the holidays approach, people relax their mitigation efforts and the third surge grows, fueled by a number of behaviors and contradictions in public health mandates from state to state. Figure 3, above, plots $R_0(t)$ using several different tabulation time spans. Note that the trends just discussed in Scenario 1a are reflected here.

$R_0(t)$, generally speaking, is greater than 1.0 when the daily changes (infections, deaths, etc.) are increasing and is below 1.0 when the daily changes have passed their peak. Note that $R_0 = 1$ does not mean that the pandemic has stalled, only that the infected people each infect just one other person on average. The total number of cases continues to increase and the number of dead continues to mount. The increase, however, is not mathematically exponential but more nearly linear. The number of available people still at risk of becoming infected decreases and so the spread necessarily dwindles as in the predator-prey problem (Younes and Hasan, 2020; Pidurkar, et al., 2021).

Note also that the curves from only three tabulation spans deviate appreciably from the average in Fig. 3. These are the longest span, 18 weeks (purple), and the two shortest spans, 2 weeks (red) and 4 weeks (orange). Calculating R_0 using 6-week and 10-week spans, as applied in Sections 4 and 5 below, gives very similar results except near the end of the run when the number of daily change counts becomes very small. We tend to favor the 6-week span for general use as this choice allows the $R_0(t)$ metric to respond quickly to abrupt changes in behaviors, mandates, and technology and yet is long enough to encompass the full progression of the disease in infected individuals. Computing R_0 in a detailed simulation is a straightforward procedure, once a particular definition is selected, because all the information is known, in practice, including who infected whom. In the real world the situation is not straightforward. One must know, ahead of time, the population's response to the evolving situation and the corresponding public health response to their changing behavior under the stress of the immediate situation, if R_0 is ever to be used to predict the course of a pandemic.

3. Computing The Basic Reproduction Number R_0

"The basic reproduction number (R_0), also called the basic reproduction ratio or the basic reproductive rate, is an epidemiologic metric used to describe the contagiousness or transmissibility of infectious agents. R_0 is affected by numerous biological, socio-behavioral, and environmental factors that govern pathogen transmission and, therefore, is usually estimated with various types of complex mathematical models, which make R_0 easily misrepresented, misinterpreted, and misapplied" (Delamater, et al., 2019). One infected person in unrestricted circulation is expected on average to lead to R_0 new cases of infection. How R_0 is measured, however, is a major source of the complexity. People, regardless of their background, generally use $R_0 > 1$ to suggest that the infection is spreading, possibly dangerously, and usually use $R_0 < 1$ to mean that the infection should be dying out. However, the words 'generally' and 'usually' imply there is a lot of room for misunderstanding and misinterpretation.

Earlier in Section 2 and in the rest of this report, $R_0(t, t_s)$ is computed as follows:

1. $R_0(t)$ is evaluated every day at midnight when the people are assumed to be at home.

2. For every person simulated, tables are kept of the person who infected them i.e. that person's permanent indices in the 'at home' MLG and the timestep when they became infected.
3. $R_0(t)$ is evaluated for 7 data tabulation time spans t_s before the current time t , to evaluate R_0 's dependence on the span. The evaluation spans used are $t_s = 2, 4, 6, 8, 10, 12,$ and 18 weeks.
4. In time span t_s before the current time t , all those infected in t_s are counted, $n_{\text{prey}}(t, t_s)$.
5. All those individuals who infected these n_{prey} are counted as $n_{\text{pred}}(t, t_s)$. This 'predator-prey' terminology describes how the epidemic works but not the single-species aspect of epidemics. An alternate 'parent-child' terminology contains a temporal, generational aspect but also implies a non-existent family relationship.
6. Many of the n_{prey} newly infected people must also be counted among a smaller group $n_{\text{pred0}}(t, t_s)$ as they are contagious as long as they have caused 0 transmissions of the virus. These contagious people should be counted in the denominator of the formula directly below with a discounted number because they have been actively contagious for only about half the tabulation time t_s .
7. The formula used here to compute $R_0(t, t_s)$ is

$$R_0(t, t_s) = \frac{n_{\text{prey}}(t, t_s)}{\left[n_{\text{pred}}(t, t_s) + \frac{1}{2}n_{\text{pred0}}(t, t_s) + \epsilon \right]}. \quad \text{Eq. (1)}$$

The factor $\frac{1}{2}$ in the formula above is an estimate of the fraction of t_s that the newly contagious person has been infected. average $R_0 \sim 1$ as the epidemic spread slows to near zero. The data structures implementing this approximation to $R_0(t, t_s)$ are efficient but still large. They also provide an important part of the computational framework needed for an efficient 'contact tracing' suite of algorithms in the future. The quantity ϵ is a small positive constant only used to protect against zero divide when the other numbers in the denominator are zero.

A number of studies have considered the evaluation and interpretation of R_0 For the Covid-19 virus. Ying Liu and co-authors, (Liu et al., 2020) consider a number of these and review the basic reproduction number (R_0) of the Covid-19 virus. " R_0 is an indication of the transmissibility of a virus, representing the average number of new infections generated by an infectious person in a totally naïve population. For $R_0 > 1$, the number infected is likely to increase, and for $R_0 < 1$, transmission is likely to die out. The basic reproduction number is a central concept in infectious disease epidemiology, indicating the risk of an infectious agent with respect to epidemic spread." They found that "the estimated mean R_0 for Covid-19 is around 3.28, with a median of 2.79 and IQR of 1.16, which is considerably higher than the WHO estimate at 1.95. These estimates of R_0 depend on the estimation method used as well as the validity of the underlying assumptions. Due to insufficient data and short onset time, current estimates of R_0 for Covid-19 are possibly biased. However, as more data are tabulated, estimation error can be expected to decrease and a clearer picture should form. Based on these considerations, R_0 for Covid-19 is expected to be around 2–3, which is broadly consistent with the WHO estimate."

R_0 is an average reproduction number but may not even gauge what is really causing the pandemic spread. "Overdispersion and super-spreading of this virus are found in research across the globe. A growing number of studies estimate that a majority of infected people may not infect a single other person. A recent paper found that in Hong Kong, which had extensive testing

and contact tracing, about 19 percent of cases were responsible for 80 percent of transmission, while 69 percent of cases did not infect another person” (Tufekci, 2020).

Let us emphasize that the basic reproduction number, R_0 , as used by epidemiologists, is not truly a parameter of the virus. It is a single number that attempts to represent the effectiveness of the virus spread in a given society, based upon the people’s behaviors, mobility, and demographics/susceptibilities at that time. For example, for a sexually transmitted disease, like HIV/AIDS, the R_0 is strongly dependent on the sexual behavior of the society. The greater the promiscuity, the higher will be the effective R_0 . One should expect R_0 to vary from city to city and country to country. We recognize that R_0 cannot be an input to the PANDEMIC simulation, but rather a statistical output calculated from the simulation. One should not attempt to define a “Covid-19” R_0 except perhaps relative to a suitable range of values averaged over representative populations, because it is not a parameter of the virus alone.

Further insight into the meaning of R_0 can be drawn from the analogous polymer system, the starburst dendrimer (Boris and Rubinstein, 1996). A starburst dendrimer is a molecule that starts from a core and adds “ R_0 ” number of monomers chemically in each subsequent generation creating a dendritic structure. The first salient observation is that you can only create dendrimers with finite numbers of generations because the number of monomers grows exponentially with generation, faster than the accessible space grows (cubically). So eventually 3-D space will not provide sufficient space for the final generation.

For an epidemic the analogous problem is that the growth of the epidemic is limited by the number of people available to be infected. This is a challenge for small-scale simulations of epidemics. If you can only simulate 1000s of people, not the millions that are actually present, then the epidemic behavior may necessarily be artificially restricted, and the outcomes potentially misrepresented by those small-scale simulations. Scaling up small simulations to approximate reality is problematic. Whenever the virus locally runs out of people to infect, either because everyone is already infected, or because vaccination has promoted immunity, the R_0 will appear to reduce. This effect is termed “herd immunity.” The speed of reaching “herd immunity” is strongly influenced by the scale of the system and the extent to which the system is one where the population is not uniformly accessible to every infected person.

There are additional factors affecting the applicability of R_0 . The nouns ‘number’ and ‘ratio’ above, instead of ‘rate’, help to hide the idea that a time-scale is involved in the definition of R_0 . Nevertheless, time is involved directly because the second word in “basic reproduction number” carries the notion of generations of infection being passed on. Realize that even the concept of ‘generation’ is potentially ill conceived if there are some true carriers who remain perpetually infectious. Pragmatically, even if the average time scale for each generation need not be specified, there is clearly a timeline involved that must be reflected in any formula being contemplated to compute R_0 . Conversely, most people contracting covid pass through a limited time cycle of infection which means there is a natural time-scale for their ability to pass the virus on. The shorter this time scale, the lower will be the resulting average value of R_0 . Finally, when there is an evolving data base, we must pick a time at which to start any calculation of R_0 .

The environment, the season, and how people adapt their behavior to cope with a dangerous infection also changes its spread. As the situation, i.e. ‘pandemic’, evolves, people’s fear, anxiety and/or boredom will be increasing, decreasing or both. As in a quantum mechanical system where the process of making a measurement changes the physical state of the system, the values

measured for the basic reproduction number R_0 at any given time are affected by the evolving response of the population and can be expected to change. This means that measurements of R_0 over limited time spans are expected to be important as seasonal and technical factors and behavioral and medical strategies change.

The population density also varies strongly from region to region, making notions of a local or even continuously varying R_0 applicable. In the same vein, the geography of a region has a major effect on the transportation technology and the mobility patterns of the populous. These are acknowledged to be important factors in how far and how fast an infection will spread. Finally changes in behavior, such as social distancing and restricting the size of meetings, are somewhat controllable factors that are continually being implemented, adjusted, and discontinued or ignored in different localities and at different times. It is these additional factors, more than the concept of R_0 or its measurement, that have motivated the development of the PANDEMIC model and this introductory study.

The next three sections report short studies in which the environmental and behavioral parameters of the PANDEMIC scenarios are held fixed for 36 weeks with only two parameters being varied. These very artificial scenarios display the intrinsic time variation of $R_0(t)$ and show how the pandemic can be controlled by simple increasing the people's mask usage and/or the percentage of time that telework replaces going to the workplace.

4. Using R_0 to Interpret Pandemic Mitigation by Masks and Telework

Figure 4 below shows the daily change plots from five simulations where the mask usage M_{eff} and the telework fraction T_{work} are increased until the pandemic has been stabilized beyond $M_{\text{eff}} = T_{\text{work}} = 0.65$. Each scenario in panels a) through e) is less unstable than the one above and the scale of daily counts at the left of the figure decrease monotonically. These five different 36-week simulations are each performed with values of $M_{\text{eff}} = T_{\text{work}}$ held fixed throughout the runs. Holding the mitigation parameters constant is the only way to demonstrate, through a relatively idealized scenario, the approximately exponential nature of the growth of the epidemic. The legend on Panel e) describes the four viral-load level interpretations of each vertical colored bar and applies for all five panels of the figure.

The top three panels a), b), and c), are arguably unstable although these three scenarios do not grown indefinitely. Each of these scenarios shows a maximum in the daily change counts after a growth period as the number of people available to be easily infected decreases. These maxima move progressively later in time as the growth rate is reduced because the mask usage and the telework fractions increase, making the uninfected people better protected. Furthermore, fewer uninfected people are being contacted due to the limits of interaction between the various networks of those in different locales and different walks of life. The panel d) simulation with $M_{\text{eff}} = T_{\text{work}} = 0.65$ is arguably a condition of marginal stability with little growth or decay of the small daily change counts. Panel e), at the bottom in Fig. 4, quite clearly is a stable condition when M_{eff} and $T_{\text{work}} = 0.70$ because all four infection levels decay away to zero by the final third of the run.

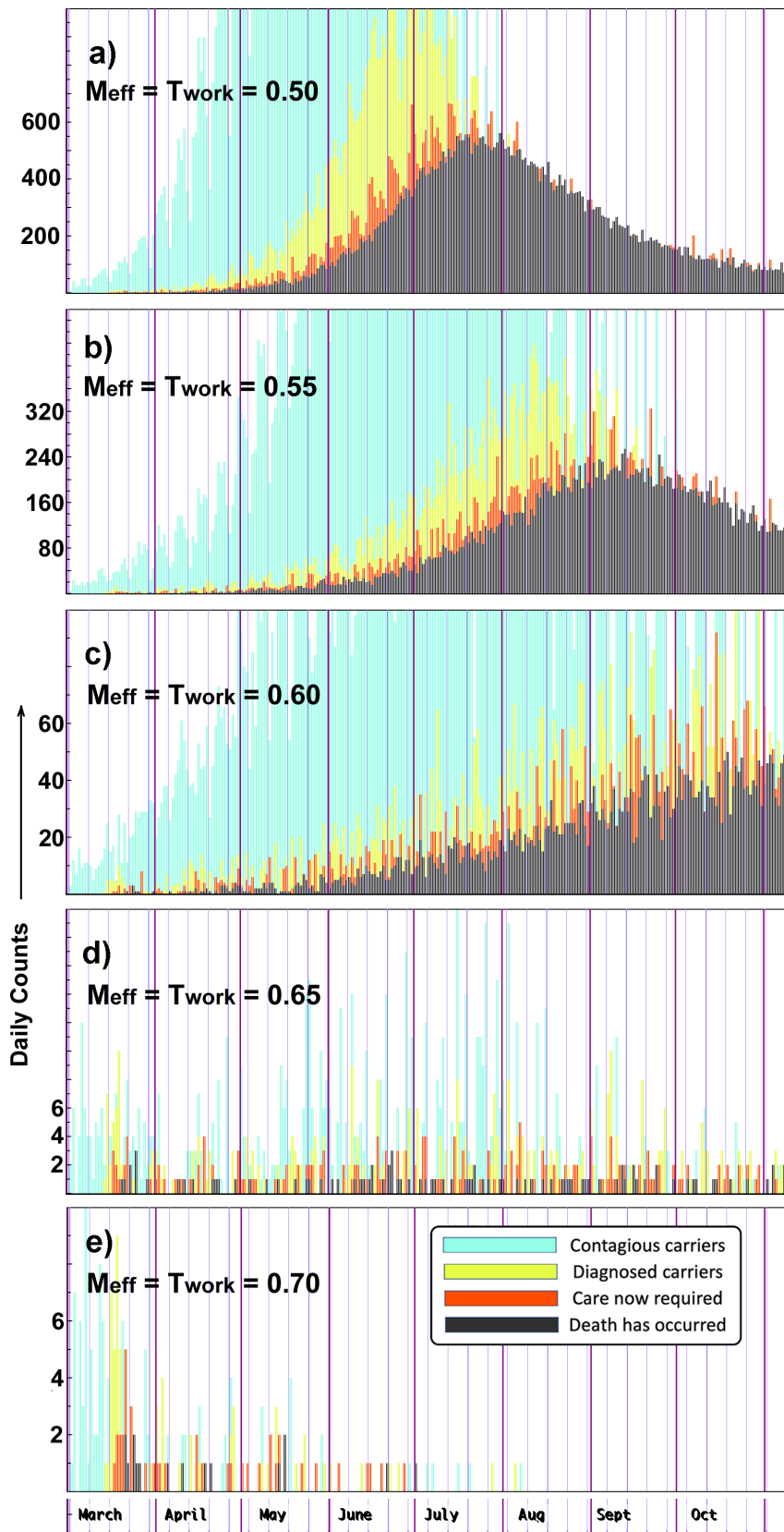


Figure 4. Daily change plots from five 36-week simulations with mask efficacy M_{eff} and telework percent T_{work} varied together as indicated above. Panel d, with $M_{\text{eff}} = T_{\text{work}} = 0.65$ approximates the marginally stable condition and the pandemic is clearly decaying in Panel e.

Figure 5 plots $R_0(t, t_s)$ versus time for $t_s = 6$ weeks and $t_s = 10$ weeks for the five scenarios from Fig. 4. There are essentially no differences in the values of $R_0(t)$ using the two values of t_s chosen. The blue curves in Fig. 5 show the basic reproduction number R_0 as a function of time for the marginally stable panel d) simulation of Fig. 4, which used $M_{\text{eff}} = T_{\text{work}} = 0.65$. The 10-week $R_0(t)$ curve is identical to the 6-week curve in Fig. 5. This set of simulations validates that $R_0(t)$ is indeed close to 1.0 at marginal stability using formula above 7.

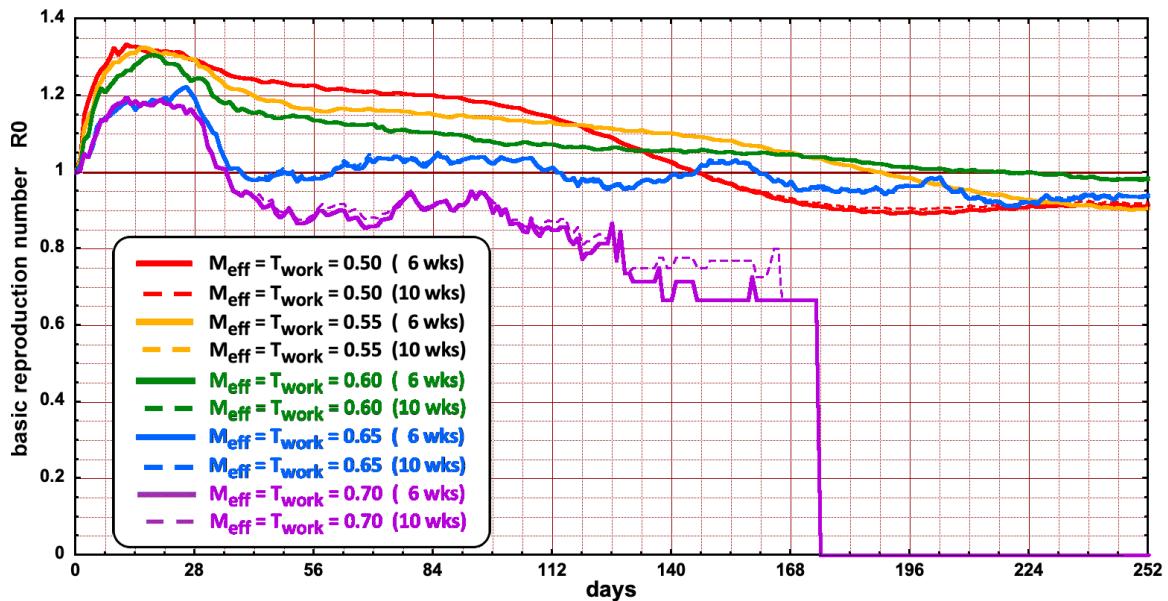


Figure 5. R_0 versus time plots from five 36-week simulations with mask efficacy M_{eff} and telework percent T_{work} varied together. M_{eff} and T_{work} % are both set at 0.50 (red), 0.55 (gold), 0.60 (green), 0.65 (blue), and 0.70 (lavender). The dashed curves, where they show for the 0.50 and 0.70 runs, are for the 10-week tabulation time span. $M_{\text{eff}} = T_{\text{work}} = 0.65$ is the approximate marginally stable condition.

Holding all the simulation parameters fixed nominally allows the possibility of exponential growth or decay of the epidemic without the influence of changes in either the people's behavior or the government's mandates. Because the number of people in any region is limited, however, exponential behavior can't persist for long. In the year-long simulation of Fig. 2 with 81 contagious people initially, approximately exponential growth continues for only about three orders of magnitude. Following a daily routine seems to naturally isolate large segments of the population from other segments. In all PANDEMIC simulations performed, the maximum total fraction of infected people was only about 15%. "WorldoMeter" records a total of about 45 million cases in the U.S. through October 2021.

The Covid-19 pandemic may be considered as a predator-prey scenario where the two competing populations, virus and people, are coupled. In the classical predator-prey system, the predator species eventually dies down to a low level when a depleted prey population becomes too small to feed a larger predator population. There are many instances of such systems including many cases in biology and chemistry. The two populations conduct a non-linearly coupled, cycle of growth and decay (Wikipedia, 2021; Lotka, 1910; J. M. Cushing, 1986; Yang, 2006). In the case of the Covid-19 pandemic, however, humans are the prey and the pandemic has not yet lasted long enough for several human generations to be born, 'consumed' by the virus and eventually replaced. Instead, the people undergo 'behavioral' generations as the society locks down and then mistakenly opens up only to lockdown again.

5. Telework Can Control an Unstable Pandemic

In Section 4 both the mask efficacy M_{eff} and the telework fraction T_{work} were held at equal fixed values throughout the simulation. In this section T_{work} is varied while the mask efficacy has the single value 0.3 through the set of five runs. Nevertheless, the system behavior as T_{work} is increased is basically the same. A large enough telework fraction can stabilize the epidemic with a marginally stable situation somewhere in between $T_{\text{work}} = 0.8$ and 0.9.

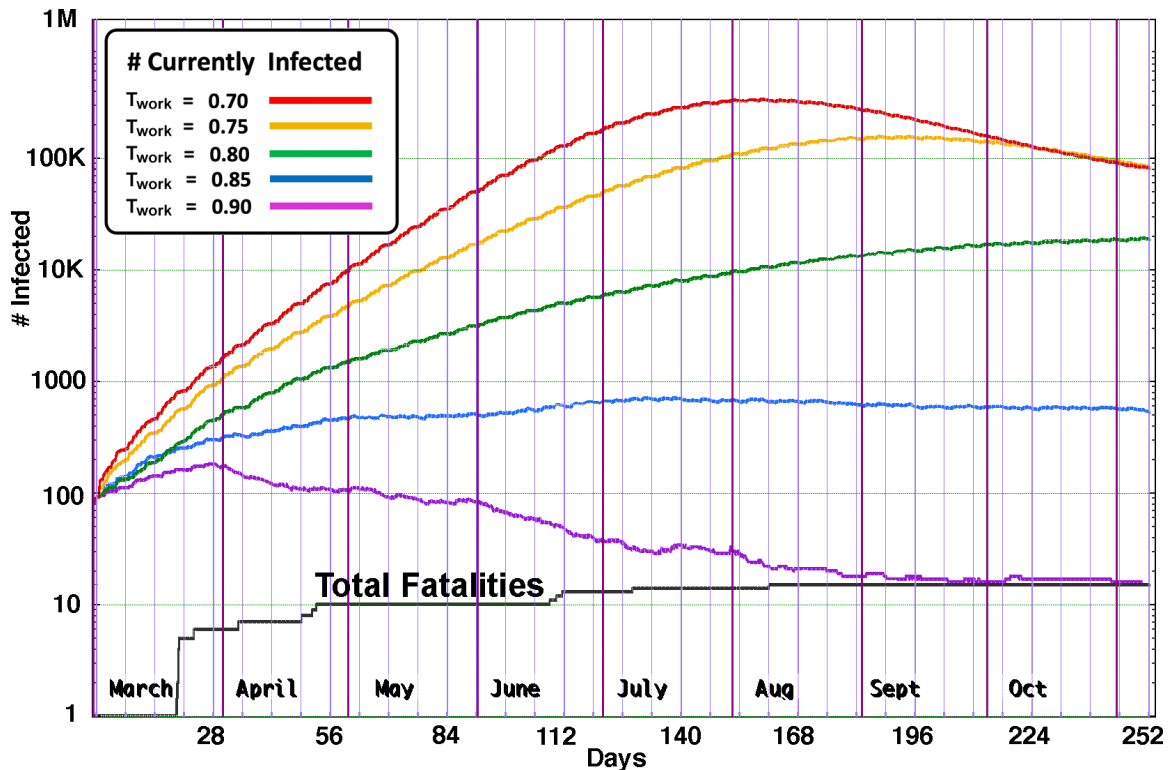


Figure 6. Telework percentage varied over a range from unstable spread of Covid-19 (red, orange and green) through marginal stability with $T_{\text{work}} \sim 0.85$ (blue) to stable (lavender). The mask efficacy is held fixed at $M_{\text{eff}} = 0.3$ for these five cases. The black curve at the bottom plots the total fatalities in the stable case, $T_{\text{work}} = 0.90$.

Figure 6 overlays the ‘contagious carriers’ curves (light blue in all the original plots) from each of five different scenarios on a single plot. The figure legend indicates the telework fraction associated with each now differently colored curve. $T_{\text{work}} = 0.70$, 0.75, and 0.80 are clearly unstable conditions. Because the mask-use effectiveness M_{eff} was only 0.3 throughout these five different cases, a correspondingly larger telework fraction is required to stabilize the virus spread. The marginally stable condition is very close to $T_{\text{work}} = 0.85$, the blue curve in Fig. 6. $T_{\text{work}} = 0.90$ (lavender curve) clearly indicates a stable/decaying pandemic after a short initial transient reflecting the initial infections.

The black curve at the bottom of Fig. 6 shows the small number of fatalities versus time that occurred in the stable scenario $T_{\text{work}} = 0.90$. This curve is seen approaching the lavender curve since all the infected people either recover (viral load disappears) or die. The only remaining viral loads above the infection level are those at the fatal level where changes in the viral load are stopped by the PANDEMIC model.

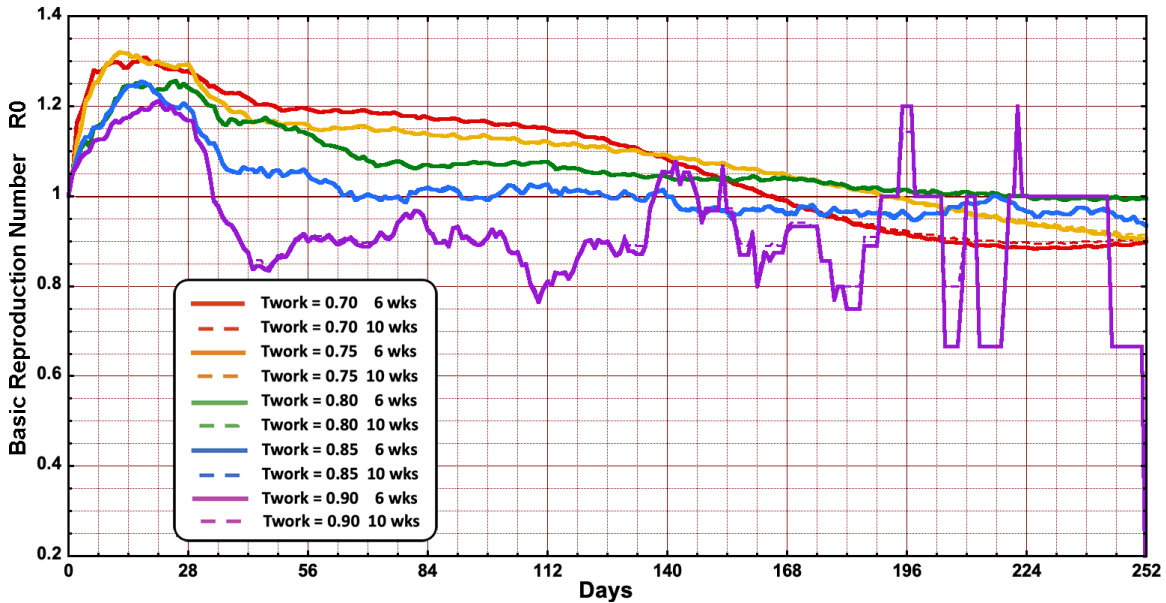


Figure 7. R0 computed for 6-week and 10-week spans for 5 values of the average telework fraction. Only the most unstable case, $T_{work} = 0.7$ and the most stable case $T_{work} = 0.9$ show small visible differences between the 6-week and the 10-week tabulation spans.

Figure 7 shows the 6-week and 10-week tabulation span computations of $R_0(t)$ for the five different telework-fraction scenarios in Fig. 6. The color scales match in the two figures. As in the results shown in Fig. 5, $R_0(t)$ drops significantly below 1.0 only in the stable case $T_{work} = 0.90$ (lavender curve). In this stable case the strong fluctuations in the second half of the run from day 125 onward arise because the number of counts is very small so changes of 1 or 2 from day to day have a significant impact on the computed R_0 . Looking at Fig. 7, it is clear that the 6-week and 10-week R_0 are basically identical. Thus the 6-week time scale is sufficient for a useful R_0 computation. Faster overall changes in parameters or overall societal strategies would be difficult to track using a 6-week R_0 definition but 6 weeks is adequate to capture most viral load evolutions in the infected persons.

6. Mask Usage Can Also Stabilize the Covid-19 Pandemic

This section summarizes a computational campaign consisting of ten 36-week scenarios in which the mask efficacy is varied while the fraction of people teleworking, T_{work} , is held fixed at 0.3. Figure 8 plots the number infected ‘contagious carriers’ with a viral load $V_L(t) > 1.0$. M_{eff} values for seven of the cases, the colored curves in the figure, span the range from 0.60 to 0.90. These values are higher than in Section 4 because the telework fraction is relatively low and contributes less to the mitigation of the virus spread.

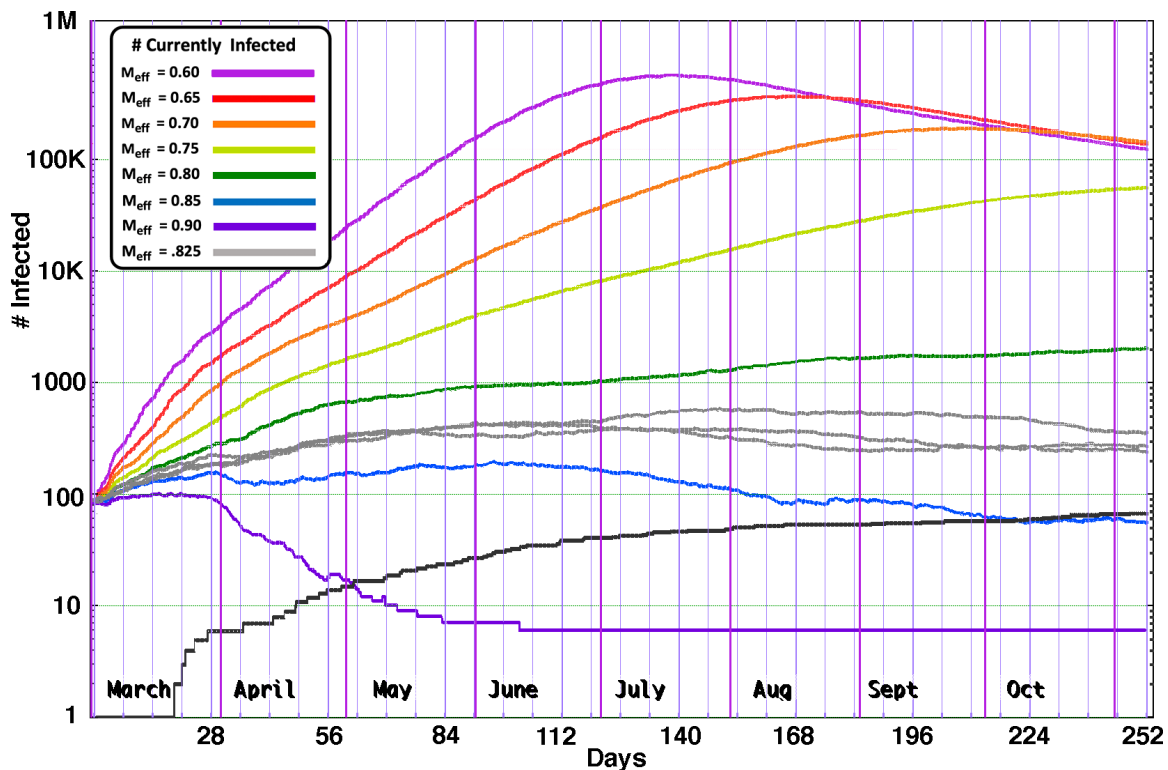


Figure 8. Number of infected people versus time includes contagious carriers but also those diagnosed, in isolation or quarantine, and those under care and fatalities. Seven values of the mask efficacy are displayed in different colors. $M_{\text{eff}} = 0.825$, close or at marginal stability, is shown in grey for an 8th case. The black curve at the bottom shows the fatalities for one of the marginally stable realizations.

In Fig. 6, where the telework fraction was being varied, the number of fatalities in the stable case, $T_{\text{work}} = 0.90$, is shown as a black curve. After 36 weeks 15 people had died. In that case the number of fatalities rose to meet the descending number of currently infected people shown as the lavender curve at the right edge of the plot. At that time the only people with measurable levels of infection were the 15 dead people. In Fig. 8, where M_{eff} is being varied, the black curve at the bottom records the fatalities for the marginally stable case, $M_{\text{eff}} = 0.825$. In this case the currently infected curve includes about 200 people who are recuperating but with viral loads still exceeding 1.0, the potentially contagious level. The number of fatalities, however, only reaches about 70 people, which is more than in Fig. 6 because the marginally stable case here involves more Covid-19 transmissions than the clearly stable case earlier.

There are three grey curves in Fig. 8, recording the results from three distinct realizations of the scenario where entirely different random numbers have been used. This variability, visible but not large, means that $M_{\text{eff}} = 0.825$ is a reasonably reliable approximation to the marginally stable mask efficacy and gives a good idea of the uncertainty expected in these simulations.

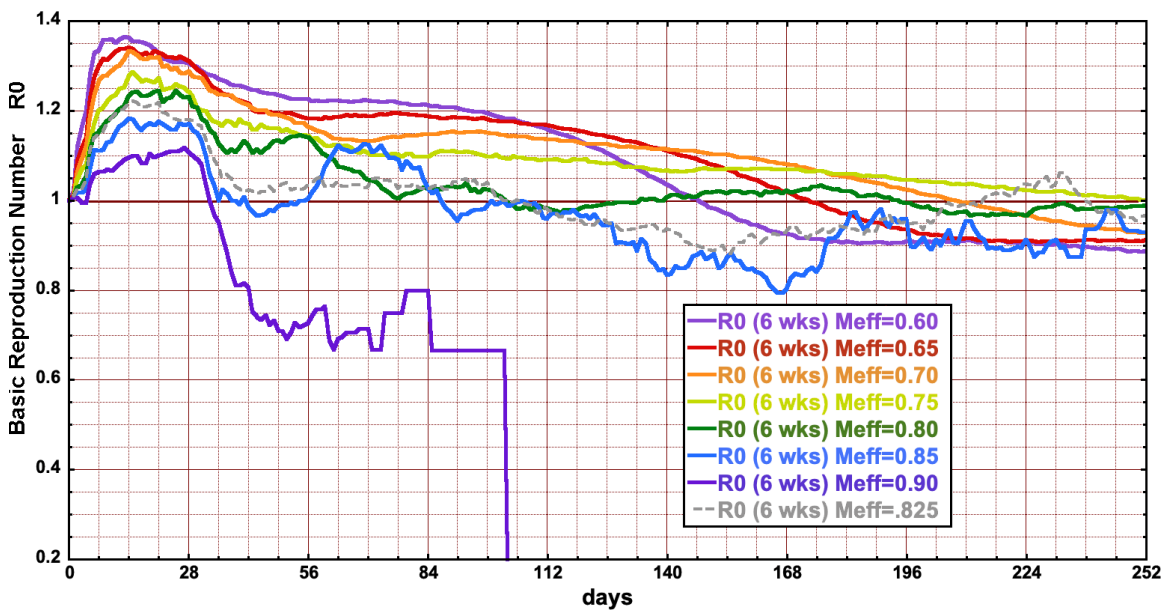


Figure 9. Basic reproduction number R_0 vs time with Mask efficacy varied. Seven runs with mask efficacy $M_{eff} = 0.60$ (magenta), 0.65 (red), 0.70 (orange), 0.75 (line), 0.80 (green – slightly unstable), 0.85 (blue – just stable), and $M_{eff} = 0.80$ (lavender). The dashed grey curve, for $M_{eff} = 0.825$, approximates the marginal stability condition, i.e. $R_0 = 1.0$. The telework percentage T_{work} was set to 0.30 for these cases.

Figure 9 just above displays the $R_0(t)$ computations for the simulations in Fig. 8 and the curves are color coded in the same way. The dashed grey curve is $R_0(t)$ for one of the realizations of the marginally stable case $M_{eff} = 0.825$. Notice that it wanders above and below the $R_0 = 1.0$ line, indicating that the calibration of the $R_0(t)$ formula described in Section 3 appears to be working. The four unstable cases, $M_{eff} = 0.60, 0.65, 0.70,$ and 0.75 , all have appreciable periods where $R_0(t)$ is greater than unity corresponding to spread of the pandemic. The value of R_0 for these unstable cases decreases in time as the positive slope of the currently infected curves in Fig. 8 decreases. $R_0(t)$ for the three most unstable cases $M_{eff} = 0.60, 0.65,$ and 0.70 drops below 1.0 as the corresponding curve in Fig. 8 pass their peaks. The lime-colored, barely unstable case $M_{eff} = 0.75$ is just leveling off by week 252 and thus drops to unity only at the right edge of Fig. 9.

7. Discussion and Conclusions

The current PANDEMIC model does not include algorithms for following the effects of vaccination or include treatments of different behaviors for different subgroups of people. A more detailed treatment could also consider the now recognized dependence of transmissibility on vaccination status, co-morbidities, and differences between indoor and outdoor venues. The model also does not yet treat in detail different regions such as states within the overall domain implementing different requirements. None of these conditions are show stoppers for the model but require implementation to generalize the model in the months since January 2021. All the capabilities and lessons learned from the Covid-19 pandemic need to be added and verified for the current situation in order that the PANDEMIC model be ready for the next epidemic.

Conclusions about R_0 drawn from the results of the three simulation campaigns presented above include:

- 1) R_0 is definitely not an intrinsic property of the virus, many other factors are involved.

- 2) The calculated R_0 is definitely time dependent and varies throughout the ebbs and flows of a pandemic, and the time span used in calculating it may have to change with the disease.
- 3) R_0 will strongly depend on the size of the system simulated as the virus inevitably 'runs out of prey.'
- 4) R_0 is strongly dependent on human behavior. Some behavior we can model like masks, telework, distancing, and gatherings. However, other more personal real world things like conversational proximity, sleep-overs visiting family, work desk proximity, shopping traffic flow, etc. have not been simulated but can impact transmission.
- 5) R_0 is a 'lagging' metric which cannot be used to predict when it is 'safe' to change behavior. That is, $R_0 < 1$ does not necessarily mean it is OK to go out again!
- 6) R_0 is strongly dependent on geographic details such as population density, mixing/mobility of subsections of the population, for instance in commuting to work, church etc, and personal proximity during transit (subway, trains, buses vs cars).

The computation of R_0 , the basic reproduction number of an epidemic, which is difficult to determine during or even after a pandemic in the real world, has been studied through simulation of several scenario sets. The examples used here compiled results over the entire area even though the behaviors and resulting incidence of infection varies from place to place. The impact of time dependence in the values of R_0 was demonstrated using a generalization of the underlying formula to consider only new infections occurring during a sliding tabulation time span of duration, t_s . The resulting curves of $R_0(t, t_s)$ show important changes in the value of R_0 in time even in idealized scenarios where all environmental and enforced behavioral parameters are being held fixed. Although the specific definition of R_0 used here seems to track the changes seen in the fundamental tabulations as a function of time, the tabulated daily change and infection plots for each scenario seem a better tool than R_0 to show what is going on and when. "In isolation, R_0 is a suboptimal gauge of infectious disease dynamics across populations; other disease parameters may provide more useful information. Nonetheless, estimation of R_0 for a particular population is useful for understanding transmission in the study population. Considered in the context of other epidemiologically important parameters, the value of R_0 may lie in better understanding an outbreak and in preparing a public health response" (Ridenhour, et al., 2014).

The detailed simulation model PANDEMIC has been demonstrated for several scenario campaigns related to the current coronavirus epidemic, Covid-19. Epidemics occur in unstable systems, which we believe is demonstrated amply by the simulations presented here. The numerical model algorithms and implementation have only been sketched in because there was more comprehensive discussion in the first two papers of the series. Frankly, the PANDEMIC model is still evolving and some aspects of the implementation may eventually be very different from the current version. There is a lot of streamlining still needing to be done for efficiency and generality. Further, the infection, immunity, and virus transmission details will certainly evolve as the current data is further analyzed.

Evolving as it has, PANDEMIC began with uncertain input parameters. Large uncertainties are to be expected in confronting a new disease. In our model we have gone for simple models that do not violate obvious constraints or information. Where uncertainty is large the model has been calibrated by multiple runs varying some computational scaling parameters to adjust the

model's response time to the overall observed rate of infections, illness, and death in the ramp up and slow-down of surges. The 'viral transmission rules of engagement' for an individual require medical research from medical experts. We have assumed that infection can only be transmitted from a contagious person to another person who is not yet contagious. Thus, two people cannot infect each other. Here are the questions we need to answer to improve our simulation:

- 1) What are the threshold viral loads that trigger: infectiousness (1.0), Symptoms (2.5), Hospitalization (3.0), requiring ventilators/critical care (3.0), and Death (3.8).
- 2) How long does it take to reach these thresholds: these times must depend on the person's age and susceptibility (randomly assigned).
- 3) What is the probability of infection as a function of distance between two people?
- 4) How does this probability change as a function of the viral load of the infected individual?
- 5) How does this probability change with time when two individuals are close together?
- 6) How does this probability change depending on the activity of the individuals, for example whether they are talking, singing or jogging?
- 7) How does this probability change when one or both are wearing a mask, m_{eff} ?
- 8) How do all of these factors change as a function of the susceptibility of the individuals (based upon factors like age, ethnicity, gender etc.)?

If these thresholds and times are probability distributions based upon the susceptibility of individuals, then the form of these probability distributions are required. In all cases, lacking hard data, the very simplest models are used subject the constraints that timescales are shorter for more susceptible people, and ultimate fatality probability agrees with demographic data.

The next large concern are the small number of individuals who may act as "super-spreaders" of a virus in a population.

- 9) What fraction of people develop only sufficient immunity to the virus to halt its progress but remain perpetually at an infectious viral load? Unknown – and modelled as zero.
- 10) What fraction of people are true symbiotic carriers, like the famous typhoid Mary, who never manifest symptoms, nor develop immunity but remain infectious indefinitely? Again unknown – and modelled as zero.

One of the strategies currently used for combatting an epidemic is to test and quarantine individuals, using contact tracing to try to quarantine potentially infected people. In order to simulate this we need to know:

- 11) Testing: What viral load is required to activate testing vis-à-vis infection?
- 12) How accurate is the viral testing; what are the probabilities of false positives and false negatives?
- 13) How many tests can be done over how much of the population? Cost?
- 14) How long does it take to return results from the test?
- 15) What % of contacts can typically be traced for quarantining?

PANDEMIC is a new model but is based on decades long development and testing of the underlying algorithms and techniques in the context of other potentially unstable systems. In an unstable system even slight changes can have profound effects if they tip the system across an unstable boundary. In the case of an epidemic or potential pandemic, randomness and

uncertainty play important roles. Near the margin between stability and instability, very small differences may have a profound effect. Thus it is important to get as far onto the stable side as possible. Just a few people acting rashly or from false information in the wrong place or at the wrong time could cause the spread of a potential epidemic to the entire system. For example, on a different version of the same day, if a plane to New York leaves the airport before a group of infected people on a bus, delayed by heavy traffic, can board the plane, thus giving airport officials, just tasked to begin testing all people planning to board, a chance to test them, there may be no ensuing pandemic at all.

Acknowledgements

Special thanks are due our colleagues Adam Moses, Gopal Patnaik, Carolyn Kaplan, Bo Cybyk and Sam Lambrakos for their important contributions over the last 35 years to the technology we have used in herding this effort forward. The research leading specifically to this capability and preliminary demonstration was supported by the projects on “Highly Complex Fluid Dynamics” and “Advanced Computational Models that Exploit Many-Core Computer Architectures” within the ONR/NRL 6.1 basic research core program.

References

- D.M. Morens and A.S. Fauci, 2013, “Emerging Infectious Diseases: Threats to Human Health and Global Stability”, *PLoS Pathogens*: **9(7)**, July 4, 2013.
- C.E. Walters, M.M.I. Meslé, and I.M. Hall, 2018, “Modelling the global spread of diseases: A review of current practice and capability” *Epidemic* **25**, pp 1-8, 2018.
- William Hanage and Helen Jenkins, The Washington Post, April 19, 2020.
- J. Boris, K. Obenschain, and D. Boris, 2021a, “PANDEMIC: To Simulate Infection Spread in a Complex Environment,” Naval Research Laboratory Memorandum Report, in review and press, NRL/MR/6003—2021/2, 17 September 2021.
- J. Boris, K. Obenschain, and D. Boris, 2021b, “Halting Covid-19: PANDEMIC - A Predictive Model to Guide Response,” Naval Research Laboratory Memorandum Report, in review and press, NRL/MR/6003–2021/3, 4 October 2021.
- A.B. Younes and Z. Hasan, 2020, “COVID-19: Modeling, Prediction, and Control,” *Applied Sciences* **10** (11), Applied Biosciences and Bioengineering section, 26 May 2020.
- S.R. Pidurkar, B. Thakran, S. Raut., L.P. Thakre, and N.V. Vaidya, 2021, “Analysis of Covid-19 in India using mathematical modeling,” International Conference on Research Frontiers in Sciences (ICRFS 2021), *Journal of Physics: Conference Series*, doi:10.1088/1742-6596/1913/1/012110.
- Wikipedia, 2021, “Lotka–Volterra equations,” https://en.wikipedia.org/wiki/Lotka%E2%80%93Volterra_equations
- Alfred J. Lotka, 1910, “Contribution to the Theory of Periodic Reactions,” *J. Phys. Chem.* **14**(3), 271–274, 1910, <https://doi.org/10.1021/j150111a004>.
- J. M. Cushing, 1986, “Periodic Lotka-Volterra competition equations,” *Journal of Mathematical Biology* **24**: 381–403, Springer-Verlag, 1986.

- X. Yang, 2006, "Uniform persistence and periodic solutions for a discrete predator–prey system with delays," *J. Mathematical Analysis and Applications*, **316**, 161–177, 2006.
- B.Z. Cybyk, E.S. Oran, J.P. Boris, and J.D. Anderson, Jr., 1994, "Application of the Monotonic Lagrangian Grid in Direct Simulation Monte Carlo Methods," AIAA Paper 94–0354, 32nd Aerospace Sciences Meeting, Reno NV, 10 – 13 January 1994, AIAA, Reston VA, 1994.
- B.Z. Cybyk, E.S. Oran, J.P. Boris, and J.D. Anderson, Jr., 1995, "Combining the Monotonic Lagrangian Grid with a Direct Simulation Monte Carlo Model," *Journal of Computational Physics* **122**(2): 323–334, December 1995.
- D. Boris, 2020, "Understanding Strategies to Protect a Populous from the Corona Virus," April 2020, see the two blogs, <https://wordpress.com/post/davidboris.wordpress.com/1077> and wordpress.com/post/davidboris.wordpress.com/1552.
- L. Bourouiba, 2020, "Turbulent Gas Clouds and Respiratory Pathogen Emissions Potential Implications for Reducing Transmission of COVID-19," *JAMA* **323**(18) May 12, 2020, <https://jamanetwork.com/journals/jama/fullarticle/2763852>.
- V. Vuorinen, Antti Hellsten, Aku Karvinen, Tarja Sironen, Peter Råback, 6 April 2020, "Researchers modelling the spread of the coronavirus emphasize the importance of avoiding busy indoor spaces," <https://www.aalto.fi/en/news/researchers-modelling-the-spread-of-the-coronavirus-emphasise-the-importance-of-avoiding-busy>.
- L. Bourouiba, E. Dehandschoewercker, J. Bush, 2014, "Violent Expiratory Events: On Coughing and Sneezing," *Journal of Fluid Mechanics* 745: 537–562, 24 March 2014, © Cambridge University Press. https://dspace.mit.edu/bitstream/handle/1721.1/101386/Bourouiba_Violent%20expiratory%20events%203-25-15.pdf?sequence=1&isAllowed=y
- California Covid Deaths by Age, 13 October 2021, (<https://www.cdph.ca.gov/Programs/CID/DCDC/Pages/COVID-19/COVID-19-Cases-by-Age-Group.aspx>, (PANDEMIC employs an earlier California table).
- P.L. Delamater, E.J. Street, T.F. Leslie, Y.T. Yang, and K.H. Jacobsen, 2019, "Complexity of the Basic Reproduction Number (R_0)", *Emerging Infectious Diseases*: **25**(1), January 2019.
- Y. Liu, A.A. Gayle, A. Wilder-Smith, and J. Rocklöv, 2020, "The reproductive number of Covid-19 is higher compared to SARS coronavirus", *Journal of Travel Medicine*: **27**(2), appeared March 2020, submitted 13 February 2020.
- B. Ridenhour, J.M. Kowalik, and D.K. Shay, 2014, "Unraveling R_0 : Considerations for Public Health Applications", *Am J Public Health* **104**(2): e32–e41. 2014 February. PMID: PMC3935673 Published online 2014 February. doi: 10.2105/AJPH.2013.301704 PMID: 24328646
- Z. Tufekci, 2020, "This Overlooked Variable is the Key to the Pandemic," *The Atlantic*, 30 September 2020.
- David Boris and Michael Rubinstein, 1996, "A Self-Consistent Mean Field Model of a Starburst Dendrimer: Dense Core vs Dense Shell," *Macromolecules* 1996 **29**, 7251–7260.